IEEE/CSC & ESAS SUPERCONDUCTIVITY NEWS FORUM (global edition), January 2016.
EUCAS 2015 preprint 2A-LS-P-03.04. Submitted to *IEEE Trans. Appl. Supercond.* for possible publication.

Comparison between Modelling and Experimental Results of Magnetic Flux trapped in YBCO Bulks

Frederic Trillaud, Kévin Berger, Bruno Douine and Jean Lévêque

***Abstract*—An electromagnetic simulation of YBCO bulks was performed and the resulting trapped magnetic flux density was compared to Field Cooling experimental measurements. Due to the underlying symmetry of the experiment and considering an appropriate set of assumptions, an axisymmetric problem relying on an A-formulation of the Maxwell's equations was solved by means of the Finite Element Method. Thus, time evolutions of measured magnetic flux densities were computed over the bulk. To express its electrical conductivity, a classic power law was adopted that included the dependence of the critical current density upon temperature and external magnetic field. This dependence was modelled on the basis of a Modified Kim-Anderson relation.**

***Index Terms*—Critical state models, trapped magnetic flux, YBCO bulk modelling.**

I. Introduction

TARGETING practical applications of High-Temperature Superconducting (HTS) bulks [1], [2], a great deal of efforts have been carried out regarding the art of growing materials, their properties and their modelling [3]–[6]. With regards to the latter, analytical formulae in the simplest 2D cases using the Bean's Critical State Model (BCSM) and numerical models in the most complex geometries, involving 3D modelling techniques and/or more refined critical current dependencies, have been developed to predict the magnitude of the penetration field and the feasibility of trapping large magnetic fluxes [7]–[9]. The present work is an incremental step in the field of HTS bulk modelling with the objective of reproducing experimental data and predicting the electromagnetic behaviour of disk-shaped samples. To that end, Finite Element Method (FEM) was applied to introduce a new critical state model based on the Kim-Anderson relation. The study is carried out under the main assumptions that bulk and background electromagnet are isotropic and homogeneous solids with cylindrical symmetry, reducing the complexity of a 3D problem to a simpler axisymmetric one. The Maxwell-Faraday and -Ampère equations were lumped into a single electromagnetic equation via the magnetic vector potential $\mathbf{A}$. In this A-formulation, the electrical conductivity of the sample was expressed through the classic power law describing the $E - J$ characteristics of HTS bulks. However, to be able to reconcile this particular formulation with an axisymmetrical model, the induced current is assumed to be solely arising from the component of the magnetic field along the axis of symmetry [10]. The resulting mathematical expression was extremized into a weak form. Subsequently, its solution was computed using the Galerkin method [11] built into the free solver GetDP of the open source software Gmsh [12], [13]. The function space is decomposed on the basis of first-order edge elements [14] and a Backward Differentiation Formula (BDF) method with an adaptive time step scheme allowed integrating the solution over space and time.

In this publication, the experimental setup used to magnetise YBCO samples under Field Cooling (FC) conditions is briefly presented followed by a detailed description of the electromagnetic model. Finally, numerical results are compared to experimental data. It is then inferred that the representation of the critical surface through a Modified Kim-Anderson (MKA) relation can approximate with high degree of accuracy the magnetisation of YBCO bulks in field cooling for a background magnetic flux density up to 3 T.

F. Trillaud is with the Institute of Engineering, National Autonomous University of Mexico, D.F., 04510 Mexico (e-mail: ftrillaudp@pumas.iingen.unam.mx)

K. Berger, B. Douine and J. Lévêque are with the University of Lorraine, GREEN, Research Group in Electrical Engineering and Electronics of Nancy - EA 4366, Faculté des Sciences et Technologies, BP 70239, 54506 Vandoeuvre-lès-Nancy Cedex, France.

Manuscript received September 8, 2015.

II. Numerical analysis

A. Experiment setup and its modelling

A disk-shaped YBCO sample prepared following a top seeded melt growth process was placed at the centre of a LHe cooled NbTi background electromagnet connected to a current-regulated DC power supply [4]. The sample was encapsulated in a copper jacket which was anchored to a 2-stage cryocooler to be cooled down to the desired operating temperature. In this setup, FC experiments were conducted at 12, 30 and 77 K on a single sample. The background magnetic field was first ramped up meanwhile the sample was in its normal-resistive state. Once the background magnetic field plateaued at its nominal value, the sample was cooled to the desired operating temperature. Then, the background magnetic field was ramped down to zero at a rate of about 0.003 T/s in order to magnetize the sample. A Hall sensor was placed at the top centre surface of the bulk to record the time evolution of the magnetic flux density. Further details of the experiment and its procedure can be found in [15]. At the rate of 0.003 T/s, the local dissipation is expected to be negligible, so the temperature is assumed to be constant throughout the magnetisation process [15].

The grid model corresponding to the experimental setup is shown in Fig. 1. It is implicitly assumed that the problem is perfectly axisymmetric with homogeneous and isotropic material properties. The model is divided in 4 regions: Ω_{m} for the background electromagnet, Ω_{b} for the sample, Ω_{s}

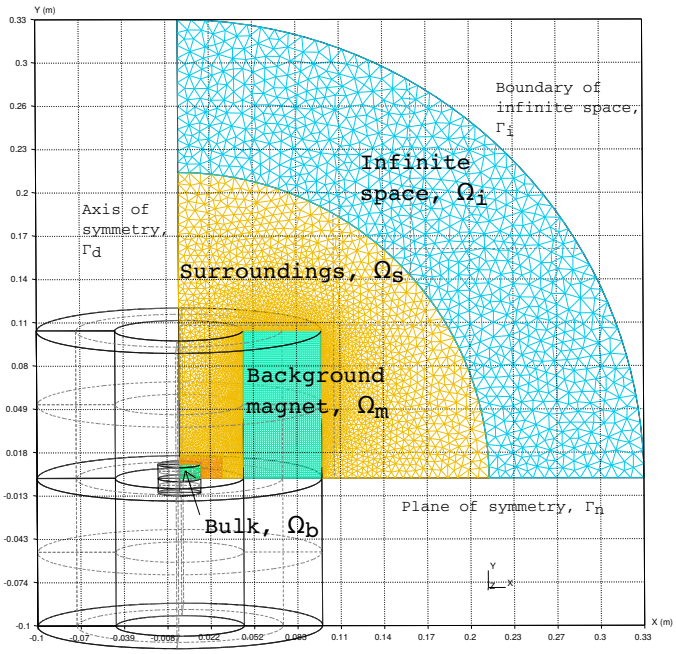

Fig. 1. Model and mesh used to compute the background and resulting magnetic flux density produced at the centre of the samples.

for the close surroundings of both electromagnet and bulk, and an additional $\Omega_{\rm i}$ region to simulate the diffusion and closing of the magnetic field in the infinite non-magnetic space surrounding the whole experiment. Table I summarizes the geometrical dimensions of the studied sample and background electromagnet. The Ampère-turns of the electromagnet were computed to match the measured intensity of the applied magnetic flux density.

B. Electromagnetic model: A-formulation

Finite Element Analysis (FEA) is proposed here to study the magnetization of YBCO bulks introducing a detailed critical state model. Amongst the body of available formulations, the A-formulation was chosen for its straightforward implementation in the solver GetDP. The basis of the model is the divergence free property of the magnetic flux density, allowing one to introduce the magnetic vector potential $\mathbf{A}$. Rewriting the Maxwell's equations in terms of $\mathbf{A}$ leads to the general expression given below

$$\nabla \times \left[\frac{1}{\mu_0}\nabla \times \mathbf{A}\right] + \sigma\frac{\partial \mathbf{A}}{\partial t} - \mathbf{J}_{\rm a} = 0, \qquad (1)$$

where $\mathbf{J}_{\rm a}$ is the imposed engineering current density flowing through the background electromagnet. The expression of the electrical conductivity of the bulk is given by the following power law expression

$$\sigma = J_{\rm c}E_{\rm c}^{-\frac{1}{n}}\left(\left|\left|\frac{\partial \mathbf{A}}{\partial t}\right|\right| + \epsilon\right)^{\frac{1-n}{n}} + \frac{1}{\rho_{\rm nsc}}. \qquad (2)$$

The introduction of $\epsilon = 10^{-6}E_{\rm c}$ in expression (2) avoids any divisions by zero when $\partial\mathbf{A}/\partial t = 0$. The normal-state resistivity was obtained from film data found in [16] and fitted to the following equation

$$\rho_{\rm nsc}(T) = 10^{-6} \times (1.6 + 0.012 \times T), \qquad (3)$$

where T is the operating temperature. The presence of the normal-state resistivity allows one to simulate the smooth transition between the normal-state resistance above the critical temperature to virtually zero resistance in the superconducting state during Field Cooling simulations as well as helping with the numerical convergence [17]. Over different numerical tries, it was noted that as the sensitivity of the numerical results upon increasing the n-values was decreasing and above 30, no significant changes could be observed. Indeed, according to (2), as the n-value gets larger and larger, the electrical conductivity becomes dependent only on the ratio of $J_{\rm c}$ and $||\frac{\partial \mathbf{A}}{\partial t}||$ as follows

$$\sigma \underset{n\to\infty}{\sim} \frac{J_{\rm c}(T,B)}{\left|\left|\frac{\partial \mathbf{A}}{\partial t}\right|\right|}, \qquad (4)$$

if one neglects the numerical terms ϵ and the normal-state resistivity $\rho_{\rm nsc}$. Thus the electrical conductivity becomes independent of n. For the following studies, values were then computed on the basis of the expression provided in [18]: 30 at 77 K, 60 at 30 K, 180 at 12 K.

It should be noted that the mathematical problem is correctly stated if the applied magnetic flux density induces a current that can freely follow the electric field without encountering any boundaries on its path [10]. It is such when the bulk is an isotropic solid with cylindrical symmetry and subjected to an applied magnetic field along the vertical axis. Hence, the current flows freely as concentric circles around the axis of symmetry and equation (1) is sufficient to describe the electromagnetic behaviour of the system without the necessity of introducing the electric scalar potential V. To simulate the infinite space that diffuses the magnetic field, a shell transformation is applied to the outer rim $\Omega_{\rm i}$ as described in [19]. Dirichlet's and Neumann's boundary conditions are applied at the edges of the model (Dirichlet: $\Gamma_{\rm i}$ and $\Gamma_{\rm d}$, Neumann: $\Gamma_{\rm n}$, see Fig. 1).

TABLE I
DIMENSIONS OF BULK AND BACKGROUND ELECTROMAGNET.

Parameters	Values (cm)
Background electromagnet	
Inner radius	5.5
Outer radius	9
Height	20
Bulk sample	
Radius	1.5
Thickness	1.67

III. Modified Kim-Anderson relation

The Kim-Anderson relation is a widely used critical state model to derive the dependence of the critical current density

upon magnetic flux density and temperature [20]–[22]. In an attempt to reproduce the experimental data over a broad range of experimental temperatures and background magnetic flux densities, the relation was altered to give the following modified version [23]

$$J_{\mathrm{c}}\left(T,B\right)=\frac{J_{\mathrm{c0}}\left(T\right)}{\left(1+\frac{B}{B_0\left(T\right)}\right)^{\alpha}}, \tag{5}$$

where J_{c0} is the temperature-dependent critical current density at zero magnetic field and α (= 0.7) is a dimensionless constant that yields the BCSM when equal to 0 and the Kim-Anderson relation when equal to 1 [24]. B is the norm of the applied magnetic flux density and B_0 is a macroscopic normalizing parameter whose temperature dependence is given by

$$B_0\left(T\right)=B_{00}\times\left[1-\delta\left(\frac{T}{T_{\mathrm{c0}}}\right)^{\beta}\right], \tag{6}$$

where B_{00}, δ and β are fit parameters, and T_{c0} = 92 K is the critical temperature. The critical current density J_{c0} was extrapolated to 0 T following a polynomial equation on the basis of the linear model given in [18]

$$J_{\mathrm{c0}}\left(T\right)=J_{\mathrm{c00}}\times\left(\frac{T-T_{\mathrm{c0}}}{T_{\mathrm{ref}}-T_{\mathrm{c0}}}\right)^{\gamma}, \tag{7}$$

The values of parameters for the best match between the numerical and experimental results over the different operating temperatures (see Fig. 3) were found to be: B_{00} = 2.67 T, δ = 1.54, β = 2.56, $J_{\mathrm{c00}} = J_{\mathrm{c0}}\left(T_{\mathrm{ref}}\right)$ = 109 A/mm^2 with T_{ref} = 77 K and γ = 0.96. To get a sense of the viability of the chosen model, Fig 2 compares the proposed critical model with data published in literature of a YBCO bulk [25]. These data correspond to a magnetic flux density applied along the c-axis. Bearing in mind that the critical surface is a unique characteristic of a given superconducting sample and that the direction of the applied magnetic field on the sample typically affects its characteristics, values of the critical current density and its general dependence on the background magnetic flux density are considered within acceptable range of sample-to-sample variabilities in quality. One of the strong key points warranting the relevancy of the modified Kim-Anderson relation in the range of the experimental measurements was that it was possible to fit accurately the experimental data of [25] up to 2 T below 77 K and up to 3 T at 77 K with the appropriate set of parameters of the MKA relation. The proposed model is an idealisation of bulk characteristics with a limited set of parameters that can only depict a smoother dependency on the applied magnetic flux density. More refined models should be considered to explore regions beyond 3 T.

IV. Comparison between Experimental and Numerical Results

Fig. 3, 4 and 5 show the different experimental measurements on the top centre surface of the bulk and the corresponding simulations. The measured magnetic flux density B_{m} was computed based on the above MKA relation (5). The induced

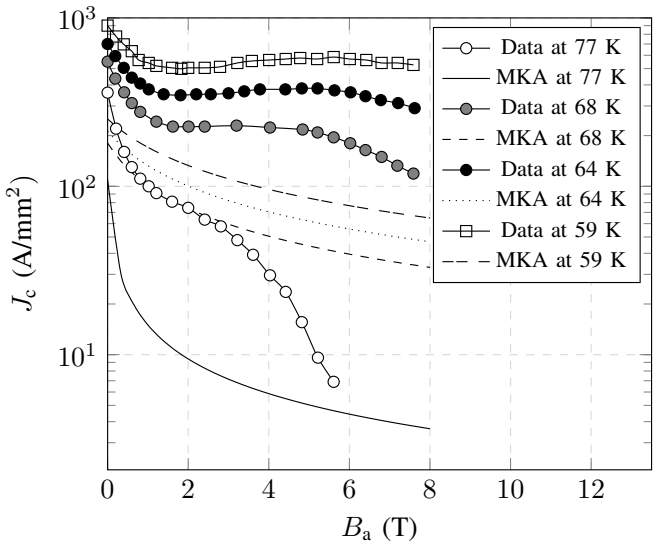

Fig. 2. Evolution of experimental critical current density of a YBCO bulk at different operating temperatures as a function of an external magnetic flux density applied parallel to the c-axis [25] compared to the proposed values obtained from the MKA relation (5). The values of the critical current densities computed with the MKA relation are lesser than the data found in literature but remain within the range of acceptable sample-to-sample variabilities arising from the manufacturing process.

magnetic flux density B_{i} generated by the bulk in response to the changing magnetic flux was derived by means of

$$B_{\mathrm{i}}=B_{\mathrm{a}}-B_{\mathrm{m}}, \tag{8}$$

where B_{a} is the norm of the background magnetic flux density. Once the background field has vanished, the measured magnetic flux density remains trapped. The largest trapped magnetic flux densities were obtained at 12 K and 30 K, amounting to nearly 77% and 68% of the nominal background magnetic flux density, respectively. However, at 77 K, the trapping is poor with only 10% of the nominal applied magnetic flux density. In terms of simulation, the proposed model reproduced fairly the behaviour of measured magnetic flux densities as well as the magnitude of the corresponding trapped magnetic flux densities throughout the different operating temperatures. At 77 K, the matching is nearly perfect whereas the computed curves at 12 and 30 K show a miscellaneous discrepancy during the decrease of the background magnetic field having a slightly rounder profile than the experimental ones. This discrepancy ought be related to the MKA relation describing J_{c} and the rate of change of the magnetic vector potential according to (5).

V. Discussion

The magnetisation curves are closely related to the evolution of the local electrical resistance of the bulk, the latter being fully defined by the parameters of the MKA relation and the rate of change of the background magnetic field. These former parameters depend on the manufacturing process and the quality of the sample. As mentioned previously, the n-value had barely any influences on the results in the range of expected experimental values which are typically several

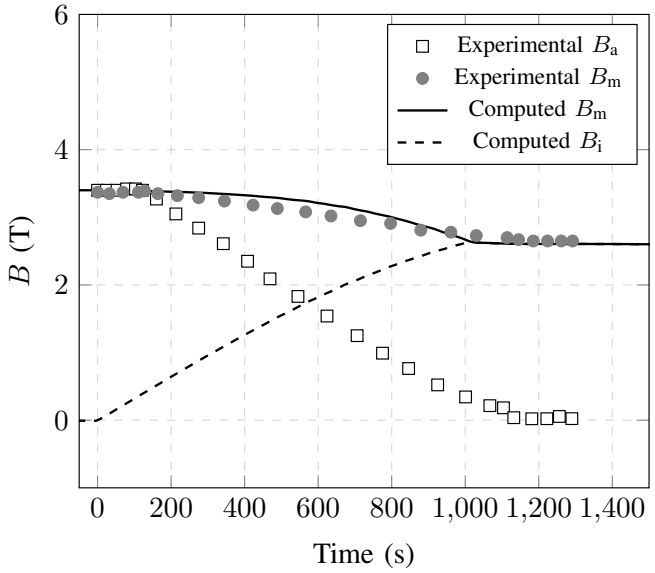

Fig. 3. Time evolution of the magnetic flux density at the top centre surface of the sample for an operating temperature of 12 K and its comparison with simulations. The square "□" and filled bullet "•" markers indicate experimental data and mark the time evolution of the background magnetic flux density B_a and measured magnetic flux density B_r, respectively. The solid "-" and dashed "- -" lines correspond to numerical simulations of the measured magnetic flux density B_m and the magnetic flux density B_i.

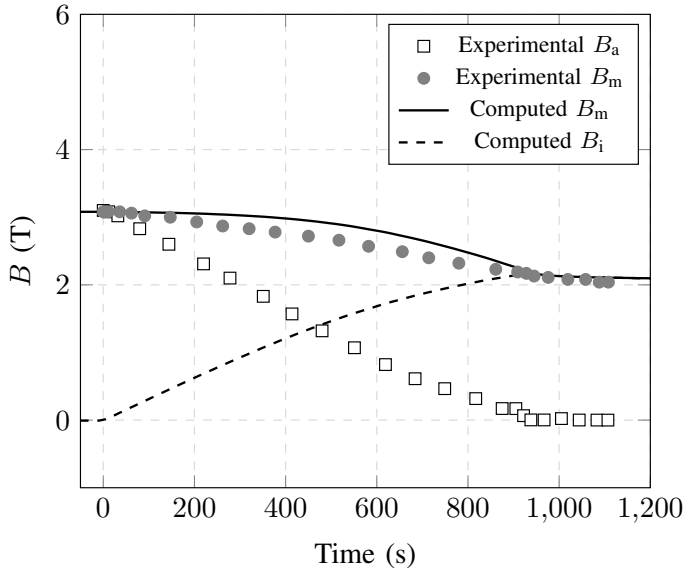

Fig. 4. Time evolution of the magnetic flux density at the top centre surface of the sample for an operating temperature of 30 K and its comparison with simulations.

tens. It becomes a free parameter that cannot be inferred from the numerical model and should be measured experimentally. Nevertheless, at low n-values (< 30), it was noted that increasing n allows trapping more magnetic flux density. In the present work, n is larger than 30. The parameters shaping the results are then mainly contained in the dependence of the critical current density upon magnetic flux density and temperature for a fixed rate of change of the background magnetic field. Thus, increasing J_{c0} and B_0 allows trapping

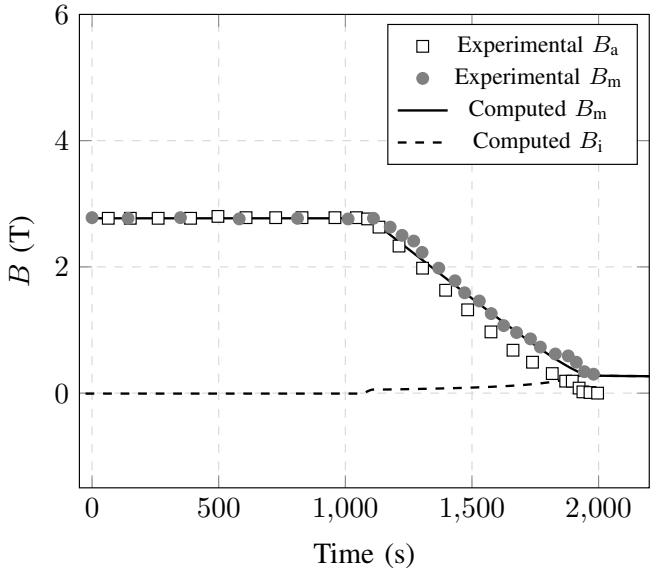

Fig. 5. Time evolution of the magnetic flux density at the top centre surface of the sample for an operating temperature of 77 K and its comparison with simulations.

more flux with a lower slope as the background magnetic field vanishes. These parameters as they are rised up modify the critical surface such that larger values of $J_{c0}(T)$ are achieved and the curves $J_c(T,\ B)$ show a lesser dependence upon background magnetic flux density than the ones presented in Fig. 2. As more data are available, it would be possible to reconstruct with greater accuracy the critical surface of the samples for background magnetic fields up to 2 T to 3 T. However, at larger magnetic flux densities, a more refined critical state model may be more appropriate and alternative fitting curves than the one proposed here with additional independent parameters might be tried out.

VI. Conclusion

The introduction of the proposed MKA relation which appears to be consistent with the expected critical surface of YBCO samples in the range of 2 to 3 T allows reproducing fairly the experimental results obtained at operating temperatures of 12, 30 and 77 T in Field Cooling conditions. The model frees the n-value which can only then be acquired through experimental measurements. The results shown that the best trapping is achieved at lower temperatures benefiting form a larger critical current density. To work with magnetic flux densities larger than 3 T, it is suggested to explore alternative critical state models with a greater degree of parametrization so that it possible to reproduce with accuracy the critical surface of the samples beyond the mentioned intensity. One of the possible methods may be to reconstruct the electrical resistivity to reproduce its magnetic behaviour and then from there derive the corresponding critical surface. This alternative approach should ultimately allow one to validate various assumptions including power law and critical state models taking into account sample-to-sample discrepancies resulting from its preparation and history.

REFERENCES

[1] L.K. Kovalev, K.V. Ilushin, V.T. Penkin, K.L. Kovalev, A.E. Larionoff, S.M-A. Koneev, K.A. Modestov, S.A. Larionoff, V.N. Poltavets, I.I. Akimov, V.V. Alexandrov, W. Gawalek, B. Oswald, and G. Krabbes, "High output power reluctance electric motors with bulk high-temperature superconductor elements," *Superconducting Science and Technology*, vol. 15, pp. 817–822, 2002.

[2] G. Malé, T. Lubin, , S. Mezani, J. Lévêque, "Analytical calculation of the flux density distribution in a superconducting reluctance machine with HTS bulks rotor," *Mathematics and Computers in Simulation*, vol. 90, pp. 230–243, April 2013. ELECTRIMACS 2011- PART I.

[3] S.B. Yan, Y.Y. Chen, H. Ikuta, and X. Yao, "Enhanced Growth Rate of a YBCO bulk in the Melt-Textured Process Under 1 atm Oxygen Pressure," *IEEE Transactions on Applied Superconductivity*, vol. 20, pp. 66–70, April 2010.

[4] W. Zhai, Y. Shi, J.H. Durrell, A.R. Dennis, Z. Zhang, and D.A. Cardwell, "Processing and Properties of Bulk YBaCuO Superconductors Fabricated by Top Seeded Melt Growth from Precursor Pellets Containing a Graded CeO_2 Composition," *Crystal Growth & Design*, vol. 15, pp. 907–914, 2015.

[5] Y. Feng, J.G. Wen, A.K. Pradhan, N. Koshizuka, L. Zhou, S.K. Chen, K.G. Wang, and X.Z. Wu, "Preparation and properties of PMP YBCO bulk with submicrometre Y_2BaCuO_5 particles," *Superconductor Science Technology*, vol. 13, pp. 703–708, 2000.

[6] Z. Hong, Ph. Vanderbemden, R. Pei, Y. Jiang, A. M. Campbell, and T. A. Coombs, "The Numerical Modeling and Measurement of Demagnetization Effect in Bulk YBCO Superconductors Subjected to Transverse Field," *IEEE Transactions on Applied Superconductivity*, vol. 18, pp. 1561–1564, June 2008.

[7] E.H. Brandt, "Superconductor disks and cylinder in an axial mmagnetic field, field penetration and magnetization Curves," *Physical Review B*, vol. 58, pp. 6506–6522, September 1998.

[8] G.P. Lousberg, M. Ausloos, C. Geuzaine, P. Dular, P. Vanderbemden, B. Vanderheyden, "Numerical simulation of the magnetization of high-temperature superconductors: a 3D finite element method using a single time step Iteration," *Superconductor Science and Technology*, vol. 22, 2009. 055005.

[9] B. Douine, C.-H. Bonnard, F. Sirois, K. Berger, A. Kameni, J. Lévêque, "Determination of j_c and n-value of hts pellets by measurement and simulation of magnetic field penetration," *IEEE Transactions on Applied Superconductivity*, vol. 25, August 2015. 8001008.

[10] A.M. Campbell, "An Introducton to Numerical Methods in Superconductors," *Journal of Superconductivity and Novel Magnetism*, vol. 24, pp. 27–33, 2011.

[11] A. Kameni, M. Boubekeur, L. Alloui, F. Bouillault, J. Lambretchs, C. Geuzaine, "A 3-D Semi-implicit Method for Computing the Current Density in Bulk Superconductors," *IEEE Transactions on Applied Superconductivity*, vol. 50, February 2014. 7009204.

[12] Patrick Dular and Christophe Geuzaine, "GetDP: a General Environment for the Treatment of Discrete Problems." [Online]. Available: http://geuz.org/getdp/.

[13] C. Geuzaine and J.-F. Remacle, "Gmsh: a three-dimensional finite element mesh generator with built-in pre- and post-processing facilities." [Online]. Available: http://geuz.org/gmsh/.

[14] R. Brambilla, F. Grilli and L. Martini, "Development of an edge-element model for AC loss computation of high-temperature superconductors," *Superconductor Science and Technology*, vol. 20, pp. 16–24, 2007.

[15] B. Douine, F. Sirois, J. Leveque, K. Berger, C.-H. Bonnard, T.-C. Hoang, and S. Mezan, "A New Direct Magnetic Method for Determining J_c in Bulk Superconductors From Magnetic Field Diffusion Measurements," *IEEE Transactions on Applied Superconductivity*, vol. 22, June 2012. 9001604.

[16] B. Wuyts, V.V. Moshchalkov, and Y. Bruynseraede, "Resistivity and Hall effect of metallic oxygen-deficient $YBa_2Cu_3O_x$ films in the normal state," *Physical Review B*, vol. 53, pp. 9418–9432, April 1996.

[17] F. Grilli, S. Stavrev, Y.L. Floch, M. Costa-Bouzo, E. Vinot, I. Klutsch, G. Meunier, P. Tixador, B. Dutoit, "Finite-Element Method Modeling of Superconductors: From 2-D to 3-D," *IEEE Transactions on Applied Superconductivity*, vol. 15, pp. 17–25, March 2005.

[18] K. Berger, J. Lévêque, D. Netter, B. Douine, A. Rezzoug, "Influence of Temperature and/or Field Dependence of the E-J Power Law on Trapped Magnetic Field in bulk YBaCuO," *IEEE Transactions on Applied Superconductivity*, no. 2, pp. 3028–3031, 2007.

[19] F. Henrotte, B. Meys, H. Hedia, P. Dular, W. Legros, "Finite Element Modelling with Transformation techniques," *IEEE Transactions on Magnetics*, vol. 35, pp. 1434–1437, May 1999.

[20] Y.B. Kim, C.F. Hempstead, A.R. Strnad, "Critical Persistent Current in Hard Superconductors," *Physical Review Letters*, vol. 9, no. 7, pp. 306–309, 1962.

[21] P.W. Anderson, "Theory of the flux creep in hard superconductors," *Physical Review Letters*, vol. 9, no. 7, pp. 309–311, 1962.

[22] P.W. Anderson and Y.B. Kim, "Hard superconductivity: Theory of motion of abrikosov flux lines," *Reviews of Modern Physics*, vol. 36, January 1964.

[23] Z. Koziol/, J.J.M. Franse, P.F. de Châtel, and A.A. Menovsky, "Magnetization of a superconductor: Results from the critical-state model," *Physical Review B*, vol. 50, pp. 15978–15992, December 1994.

[24] S. Tochihara, K.-I. Harashima, H. Yasuoka, H. Mazaki, M. Osada, M. Kakihana, "Temperature Dependence of Lower Critical Fields in a single-Crystal $Bi_2Sr_2CaCu_2O_{\delta+d}$ Bulk Superconductor," in *Advances in Superconductivity X: Proceedings of the 10th. International Symposium on Superconductivity (ISS'97)* (K. Osamura and I. Hirabayashi, ed.), vol. 2, pp. 63–66, Springer, October 1997. ISBN: 978-4-431-66881-7.

[25] G. Krabbles, G. Fuchs, W.-R. Canders, H. May, R. Palka, *High Temperature Superconductor Bulk Materials: Fundamental, Processing, Properties Control, Application Aspects*. Wiley-VCH, 2006. ISBN: 978-3-527-40383-7.